

Dielectrophoretic Separation of Cells Using 3-D Microelectrode

Zurina Zainal Abidin^{1*}, Zalini Yunus² and Gerard H. Markx³

¹Department of Chemical Engineering and Environmental,

Faculty of Engineering, 43400 UPM, Serdang, Selangor, Malaysia

²STRIDE, MINDEF, Taman Bukit Mewah Fasa 9, 43000, Kajang, Selangor

³School of Chemical and Analytical Science, University of Manchester,

Sackville Street, M60 1QD, Manchester, UK

*E-mail: zurina@eng.upm.edu.my

ABSTRACT

The dielectrophoretic (DEP) separation of cell, using microelectrodes structure, has been limited to small scale due to size of the substrate. This work was carried out to extend the capability of microelectrodes system by orientating the microelectrodes in three dimensions (3-D) for larger scale dielectrophoretic separation of microorganism. The designed 3-D separation chamber consists of microelectrodes on two opposing walls. Based on the FEMLAB simulation, the electric field was seen to be generated across the chamber, rather than between adjacent electrodes in the same plane like in the small scale system. This configuration led to a stronger electric field in the bulk medium. The experimental results showed that the 3-D microelectrodes chamber behaved similar to the system with microelectrodes on one wall. The effects of the main parameters such as voltage, frequency and flow rates were similar to that of the systems with all the electrodes on one wall, but on the overall, capture more cells. A gap size between 250 – 500 μm resulted in an electric field which is strong enough to hold cells while giving a reasonable cross sectional area at the same time. Although there is some improvement achieved by 3-D system, it is still not very much, as compared to the small scale system.

Keywords: 3-D, dielectrophoresis, cell separation, microelectrodes

NOMENCLATURE

ϵ_p^*	Complex dielectric permittivities of the particle (F/m)
ϵ_m^*	Complex dielectric permittivities suspending medium (F/m)
F_{DEP}	Force of DEP (N)
r^3	radius of particle (m)
ϵ_0	free space permittivity (F/m)
ϵ_m	medium permittivity (8.854×10^{-12} F/m)
$Re(fcm)$	real part of the Clausius-Mossotti factor
∇E^2	Square of the electric field gradient (V^2/m^3)
j	imaginary number

INTRODUCTION

Advances made in many bio-related areas, such as cell biology, bioprocessing and others, have generated a demand for highly efficient and improved cell separation techniques. The manipulation of the behaviour of a particle or cell in a non-uniform electric field or also known as dielectrophoresis (DEP) (Pohl, 1978; Pethig, 1996) is one of the promising methods available to be explored. The

Received: 4 April 2008

Accepted: 16 May 2008

*Corresponding Author

particle or cell can exhibit positive or negative DEP when suspended in a fluid medium, due to the dipole associated with charge distribution at the fluid/particle interface. Dielectrophoresis has shown many applications, such as in monitoring and purifying cell cultures (Becker *et al.*, 1994; Docoslis *et al.*, 1994; Markx *et al.*, 1994a), detection and removal of toxic pathogens from water (Suehiro *et al.*, 2003), separation of dead and live cells (Li *et al.*, 2002; Markx *et al.*, 1994b) as well as removal of human breast cancer from CD34+ from stem cells (Huang *et al.*, 1999). The DEP has the advantage of being non-invasive and can be conducted under sterile conditions. More importantly, DEP can be integrated with other methods to achieve improved separation since the physical properties exploited this technique has little impact on the other cell separation methods.

Currently, the DEP makes use of microelectrodes which are fabricated using photolithography technique. The high field intensities, which are important for the DEP application, have become possible due to the small dimensions of the microelectrode. Furthermore, it reduces the heat and enhances heat dissipation. However, the size of the substrate limits the capability of the microelectrodes to microlitres. This is rather unattractive for industrial application, which requires more sample volumes to be processed.

In most separations, the microelectrodes are only on one planar plate. The effective surface area of electrodes has also been reduced because only one side of the chamber is typically covered with electrodes. It is theoretically possible to scale up the DEP separations using large electrodes and electrical potentials. In practice, this may however cause electrical heating and electrochemical effects which can reduce the DEP effect and kill the cells.

In this work, the main aim was to extend the microelectrodes capability by orientating the microelectrode in 3-D arrangement and investigate its effectiveness for larger scale DEP separation of cells. Furthermore, this study also served as a basis in determining the important characteristics for scaling process.

THEORY

Dielectrophoresis works because of the existence of the non-uniform AC electric field, which is vitally determined by the electrode configuration. Following established theory (Pohl, 1978; Pethig, 1979; Jones, 1995), the DEP force, F_{DEP} acting on a spherical particle of radius r , suspended in a fluid of absolute dielectric permittivity, ϵ_m is given by:

$$F_{DEP} = 2\pi r^3 \epsilon_0 \epsilon_m \text{Re}(f_{cm}) \nabla E^2 \quad (1)$$

where $\text{Re}(f_{cm})$ is the real part of the Clausius-Mossotti factor, ∇E^2 is the square of the electric field gradient, ϵ_m is the medium conductivities and ϵ_0 is the free space permittivity ($8.854 \times 10^{-12} \text{ Fm}^{-1}$).

$$f_{cm} = \frac{(\epsilon_p^* - \epsilon_m^*)}{(\epsilon_p^* + 2\epsilon_m^*)} \quad (2)$$

where ϵ_p^* and ϵ_m^* are the frequency-dependent complex dielectric permittivities of the particle and its suspending medium defined by:

$$\epsilon_p^* = \epsilon_p - j \frac{\sigma}{\omega} \quad (3)$$

where ϵ_p are the permittivity of the particle and its suspending medium. σ is the conductivity, ω is the angular frequency, ($\omega = 2\pi f$) and $j = \sqrt{-1}$. The Clausius-Mossotti factor is a measure of the strength of the effective polarization of a spherical particle as a function of particle and medium permittivity. Clausius Mossoti factor is dependent on the applied frequency and also the electric properties of the particle relative to the medium. Theoretically, it should have a value between +1.0 to -0.5, which means that the DEP force can be positive and negative.

MATERIALS AND METHODS

Electric Field Simulation

FEMLAB 2.3 (Comsol Ltd) was used to simulate the electric field generated by the designed electrode systems. The FEMLAB is based on finite element analysis and partial differential equations. The module used was electromagnetic module, and the electric field calculation was done in 3-D.

The chromium electrodes were modelled as a layer with 100 nm thickness, placed onto a glass substrate of 50 μm thickness. Water with electrical permittivity of 78 was used as the medium and projected as a layer of 200 μm thickness. Both the glass substrate and water were considered as insulators. All simulations were done at voltages ranging from 2-20 V_{peak-peak} and at a frequency of 1 MHz.

Micro-organism Preparation

The yeast used was *Saccharomyces cerevisiae* (strain 239, isolated from Whitbread the brewers, and obtained from Mr. Ralph Cooper, University of Manchester). It was grown overnight in a 100 ml MYGP broth containing 0.3% each of yeast and malt extracts (Oxoid), 1% of glucose and 0.5% of mycological peptone (Oxoid), at 35°C in an orbital shaker with a speed of 150 rpm. The cells were centrifuged (Int. Equipment, model Centra 4MPR), washed four times and re-suspended in deionised water to reduce the conductivity. After that, the conductivity was checked using a Jenway conductivity meter (model 4010). The concentration of the cells was measured using a UV spectrophotometer (PYE Unicam 8600, Philips) in a cuvette of 1 cm path length before carrying out the experiments.

Fabrication of Microelectrodes

The microelectrodes were fabricated using a standard photolithography method described previously (Markx *et al.*, 1994a). Microelectrodes were made from chromium on a glass surface (75 mm x 25 mm) in the clean room at the School of Electronic and Electrical Engineering, University of Manchester. Interdigitated parallel microelectrodes, which were drawn using AutoCAD 2002, were used to study the effectiveness of the 3-D microelectrodes system. These microelectrodes have a width of 50 μm , while the distance between the adjacent electrodes was also 50 μm .

A chamber was then prepared to carry out the DEP separation experiments. In this work, the chamber made was similar to those described by Markx and Pethig (1995). A 3-D separation system was obtained by sandwiching a Teflon spacer (50 μm depth) between two glass plates with microelectrodes which were placed opposite each other. The final depth of the chamber was found to be around 250 μm (*Fig. 1*).

Experimental Procedures

The equipment used in this study is shown schematically in *Fig. 2*. The DEP chamber was placed on top of the microscope to monitor the behaviour of cell. A Nikon camera was mounted onto the microscope (Eclipse E600) and deionised water was continuously fed into the chamber using

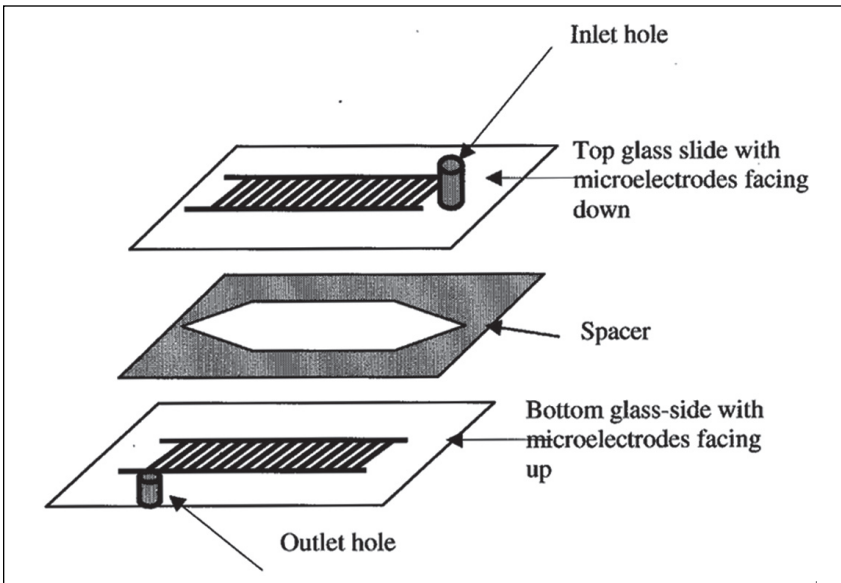


Fig. 1: Schematic presentation of dielectrophoretic separation chamber for 3-D system

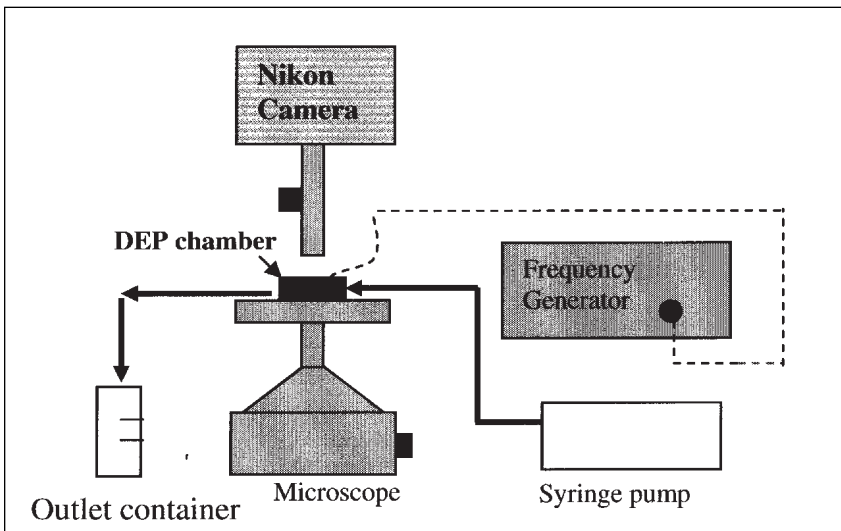


Fig. 2: Flow diagram of the system used for the dielectrophoretic separation of cells

a 10 ml syringe, which was controlled by a Sage instrument syringe pump (Model 355, Sage Instruments, USA). A measuring cylinder was placed at the outlet to collect the cell and water mixtures. Before the start of the experiments, the concentration of the cells was determined using the spectrophotometer (PYE Unicam, Philips; model 8600) at 660 nm. The optical density was adjusted until it achieved a value of 1.8 (equivalent to 2.8×10^8 cells per ml). The medium conductivity was $5 \mu\text{Scm}^{-1}$.

Water was let flowing into the DEP chamber prior to the introduction of the cells. The electric field was applied to the electrodes using a frequency generator (Thurlby Thandar Instruments, model TG120). Next, a pulse of cells was injected at the inlet tubing, using a syringe and the water went through the chamber was maintained to wash away the cells which were not attracted to the electrodes. After one hour, the experiment was stopped and the outlet suspension was collected to measure the optical density.

RESULTS AND DISCUSSION

In this work, two microelectrodes planes were placed opposite each other, top and bottom, and were energized with electric field. This resulted in an electric field pattern which acted between the bottom energized electrode and the top grounded electrode. The strongest electric field was found at the edges of the electrodes, while the strength of the field was found weaker away from the edges. *Fig. 3* shows the results of the FEMLAB analysis carried out for the electric field of the 3-D chamber at $x = 1.5 \times 10^{-4}$ m for 250 μ m gap size at $8 V_{pk-pk}$. The magnitude of the largest electric field strength is 2.8×10^4 Vm^{-1} at the edge of bottom electrode. The strength of the electric field declined further away from this edge before it started to peak again somewhere near the top electrode plane with a magnitude of about 1×10^4 Vm^{-1} .

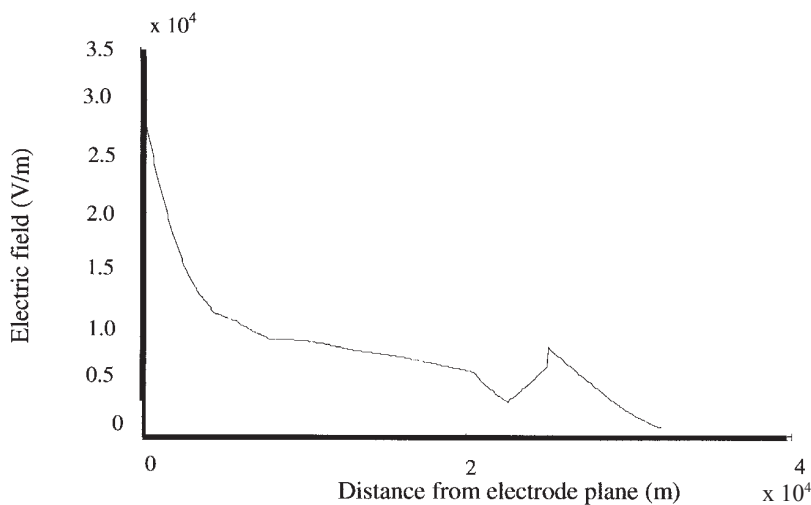


Fig. 3: The electric field pattern variations at $x=1.5 \times 10^{-4}$ m for 250 μ m gap size at $8 V_{pk-pk}$ in z -direction. The electric field is decaying from a peak value as the distance increases. However, near the top electrode the electric field increases back slowly and reached another peak

In a system with only one wall covered with planar microelectrodes, the electric field was generated between the neighbouring electrodes in the same plane, and then decayed exponentially as a function of the height above the electrode plane (Markx *et al.*, 1994b). For the system with opposing electrodes, in which the electric field was generated across the chamber, the electric field pattern was found to penetrate further into the chamber cross section, and hence the likelihood of a particle being caught in a high field region was also higher. These findings suggested that using a chamber having opposing microelectrodes could be better than using the chamber based on electrode arrays with adjacent microelectrodes. However, it should be noted that the gap between opposing

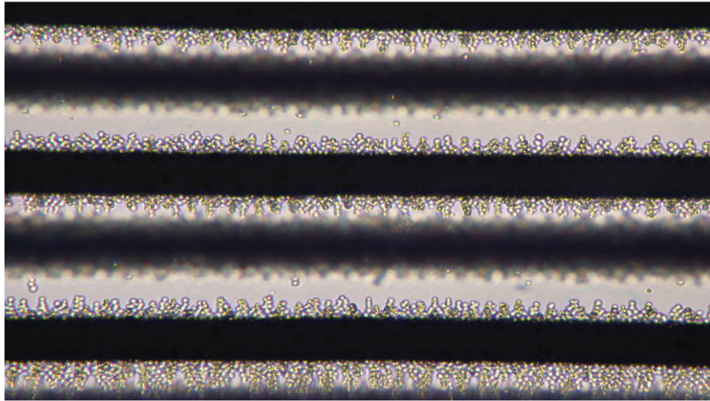


Fig. 4: Yeast cells collected at the electrode edges of both top and bottom electrodes. The applied voltage and frequency were 8V peak to peak and 1 MHz. The gap of the chamber used was 250 μm . The distance between the top and bottom neighbouring electrodes was 150 μm . The blurred arrays are the top array. The picture was taken at 20x magnification

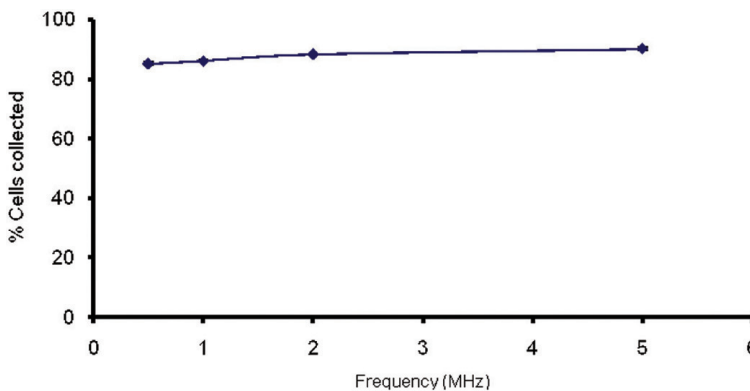


Fig. 5: The percentage of cells collected increases non-linearly as a function of the applied frequency

microelectrodes was quite large, and in this case, it was at least 250 μm between the electrode planes and 150 μm in the planes. As a result, it should be no surprise that the electric field values, in the opposing electrode system, were likely to be smaller than those in the system with adjacent microelectrode, in which the distance between the adjacent electrodes was typically 50-150 μm .

In this work, a simple 3-D separation chamber was constructed and a set of experiments was carried out to determine the performance of the new DEP chamber. The investigation was started by varying the applied frequencies, while setting the voltage and flow rate at 8 V_{pk-pk} and 9 $\mu\text{l min}^{-1}$, respectively. The gap size between the top and bottom electrodes was 250 μm , and the medium conductivity was 5 $\mu\text{S cm}^{-1}$.

Fig. 4 demonstrates a typical collection pattern of yeast cells under the influence of 1 MHz applied frequency and 8V_{pk-pk}. These yeast cells were seen to be collected at the electrode edges of both the top and bottom electrodes. When the frequency was increased from 0.5 MHz to 5 MHz, the number of cells attracted to the electrodes increased (Fig. 5). Nearly 85% of cells were found

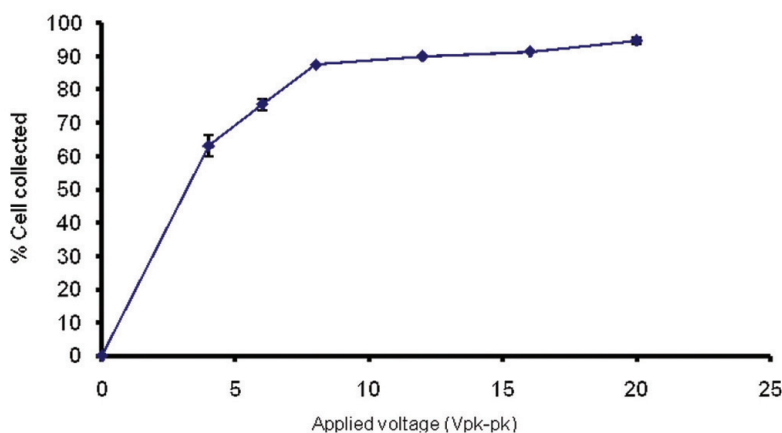


Fig. 6: Changes in the percentage of the cells collected at an applied voltage of $8 V_{pk-pk}$. The percentage of the cells collected increases as the voltage increases

to be attracted at 0.5 MHz, and this was around 91% at 5 MHz. This was in concordance with the previous findings by Huang *et al.* (1992). However, pearl chain formation, which could be of advantage in capturing the other cells, was found to be less at 5 MHz than around 1 MHz.

In the next set of experiments, the voltage was varied from 2 to 20 V_{pk-pk} at 1 MHz and $9 \mu\text{l min}^{-1}$. When there was no electric field, no cells were collected. Once the electric field was applied, the result (Fig. 6) showed that as voltage increased, the percentage of cells attracted to the electrodes was also increased. Nearly 65% cells were already collected at 4 V_{pk-pk} . At low voltages, the fluid drag force exerted onto some of the cells was often larger than the magnitude of the DEP force holding them. When the voltage increased, the magnitude of the electric field strength as well as the DEP force holding the cells at the electrode had also increased and resulted in less cells being washed away from the chamber.

The next investigation conducted was varying different flow rates from $9 \mu\text{l/min}$ to $193 \mu\text{l/min}$. The gap between the slides in the separation chamber was $250 \mu\text{m}$ at 1 MHz and $8 V_{pk-pk}$, respectively. Fig. 7 illustrates that the percentage of cells attracted to the electrodes decreased as the flow rates became faster. This was rather expected because increasing the flow rates would in turn increase the drag force exerted on the cells, whilst the DEP forces holding the cells at the electrodes remained constant. Hence, more cells were flushed out from the separation chamber when the flow rate was increased. The flow in the DEP chamber would have a parabolic velocity profile. Therefore, the drag force would virtually be zero at both of the electrode planes and this was the maximum at the middle of the chamber. This contradicted the DEP force, which would be at its maximum at the electrode plane and minimum in the middle of column. It is believed that only cells which reside at the middle of chamber are likely to be washed away.

When scaling up, it is desirable to process as much sample volume as possible. One way of doing this is by increasing the cross sectional area of the chamber. This allows more sample volume to be handled at one time. The next experiments were carried out by varying the gap of chamber, i.e. from $250 \mu\text{m}$ to 1 mm at 1 MHz and $8 V_{pk-pk}$. Increasing the cross sectional area of the chamber was found to reduce the velocity. Thus, in order to maintain the velocity of the fluid flows for all the different gap sizes, different flow rates had to be used. The velocity needed to wash the cells

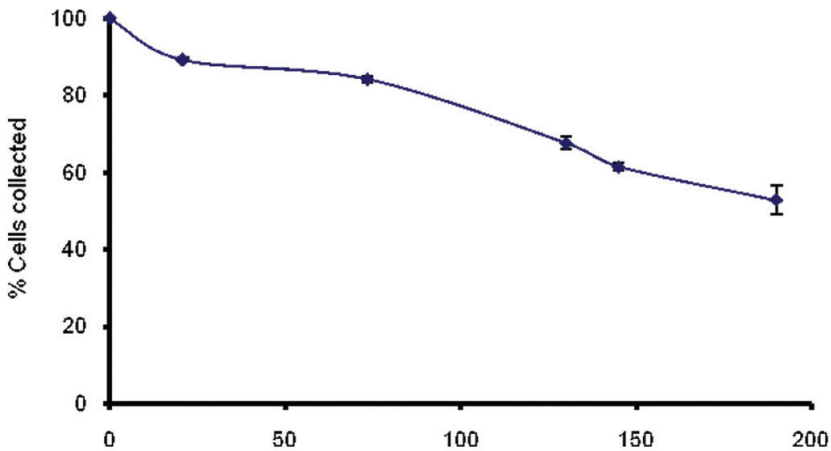


Fig. 7: The influence of the flow rate on the number of cells attracted to the electrodes. More cells are flushed out from the separation chamber at higher flow rates since increasing the flow rates will increase the drag force

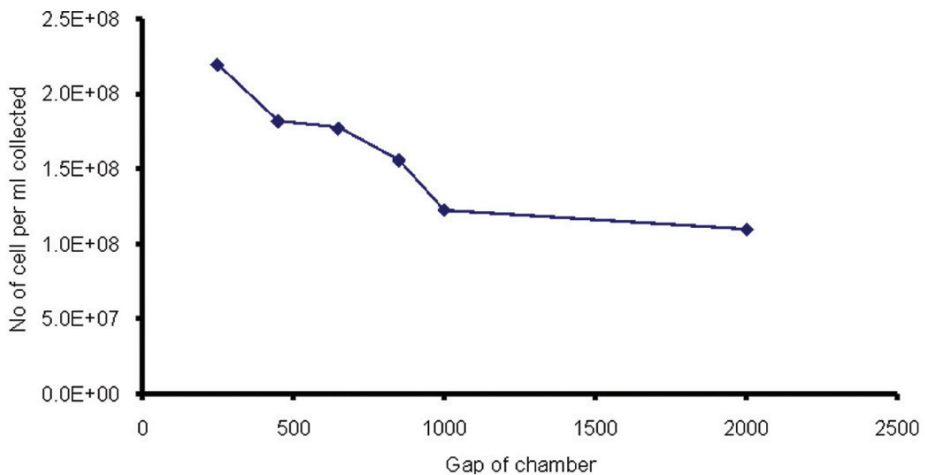


Fig. 8: The influence of the gap between the top and bottom electrodes on the number of cells attracted to the electrodes. The number of cells collected at the electrodes decreases as the gap increases

that were not attracted to the electrodes was determined for each electrode gap experimentally. The gaps used were 250 μm , 450 μm , 600 μm , 800 μm , 1000 μm , 2000 μm , 6000 μm and 10000 μm . The corresponding flow rates were 9 $\mu\text{l min}^{-1}$, 18 $\mu\text{l min}^{-1}$, 90 $\mu\text{l min}^{-1}$, 180 $\mu\text{l min}^{-1}$, 420 $\mu\text{l min}^{-1}$, 800 $\mu\text{l min}^{-1}$, $\sim 24 \text{ ml min}^{-1}$ and $\sim 100 \text{ ml min}^{-1}$, respectively.

The results, shown in Fig. 8, indicate that the number of cells attracted to the electrodes decreased as the gap between the electrodes was increased. This is entirely due to the higher DEP force experienced by the cells, as the gap decreases. At 250 μm , these cells were observed to be attracted to both the top and bottom electrodes. However, as the gap between the electrodes was

increased to 450 μm , less cells were collected, and most of them resided at the bottom electrodes. The number of cells collected further reduced as the gap was increased to 650 μm , 850 μm , 1000 μm and 2000 μm . At 250 μm and 450 μm , the pearl chains formed by the cells were still distinct. As the gap sizes increased, pearl chain formation was less, and the cells were also more dispersed.

The bigger the gap size, the more volume sample can be processed. The above results suggest that the electric field interaction between the top and bottom electrodes will only be effective throughout the length of chamber or bulk medium for collection of cells up until a certain gap size of around 600 μm . This also means that although a bigger gap between the interacting electrodes would help process more sample volume, the effectiveness of the electric field throughout the bulk medium was reduced and hence the collection of cells. The further away the cells into the bulk medium, the drag force will be larger than the DEP force and flushes them away to the outlet. It therefore, limits the capability of this 3-D microelectrode system.

CONCLUSIONS

An extension to photolithographic approach was attempted for the DEP separation at larger scales. A 3-D separation chamber was designed with microelectrodes on two opposing walls, with the electric field generated across the chamber, rather than between the adjacent electrodes in the same plane like in the small scale system. The experimental results showed that this system behaved similar to the systems with microelectrodes on one wall, but it captured more cells. This configuration led to a stronger electric field in the bulk medium. In the experiments it performed well, giving substantial amount of cell collection. The experimental results also showed that the effects of the main parameters such as voltage, frequency and flow rates were similar to that of the systems with all the electrodes on one wall. A gap size between 250 – 500 μm gave the best results. However, in comparison to the small scale system, the improvement was still not very much. This result has a big implication in that it limits the capacity of the microelectrode system. The findings from this study also suggest that in scaling up dielectrophoretic separation, it is very important for the electrode to generate high electric field strength in the system. The electrode system must be able to fully utilized the surface area of the electrode and also rapidly dissipate any heat generated within the system. The findings also suggest the possibility of using a different approach from the conventional photolithography technique to ensure success in scaling up.

ACKNOWLEDGEMENT

We wish to thank Universiti Putra Malaysia for its financial support.

REFERENCES

- Becker F.F., Wang, X.B., Huang, Y., Pethig, R., Vykoukal, J. and Gascoyne, P.R.C. (1994). The removal of human leukaemia cells from blood using interdigitated microelectrodes. *Journal of Physics D: Applied Physics*, 27, 2659-2662.
- Docoslis A., Kalogerakis, N., Behie, L.A. and Kaler, K.V.I.S. (1994). A novel dielectrophoresis-based device for the selective retention of viable cells in cell culture media. *Biotechnology Bioengineering*, 54, 239-250.
- Huang Y., Holzel, R., Pethig, R. and Wang, X.B. (1992). Differences in the AC electrodynamic of viable and non-viable yeast cell determined through combined dielectrophoresis and electrorotation. *Physical Medical Biology*, 37, 1499-1517.
- Huang Y., Yang, J., Wang, X.B., Becker, F.F. and Gascoyne, P.R.C. (1999). Cutting edge communication: The removal of human breast cancer cells from hematopoietic CD34+ stem cells by dielectrophoretic field-flow-fractionation. *Journal of Hematotherapy and Stem Cell Research*, 8(5), 481-490.

- Jones, T.B. (1995). Dielectrophoretic force calculation. *Journal of Electrostatics*, 6, 69-82.
- Li, H. and Rashid, B. (2002). Dielectrophoretic separation and manipulation of live and heat-treated cells of *Listeria* on microfabricated devices with interdigitated electrodes. *Sensors & Actuators: B.*, 86(2-3), 215-221.
- Markx G.H., Huang, Y., Zhou, X.F. and Pethig, R. (1994a). Dielectrophoretic characterization and separation of microorganism. *Microbiology*, 140, 585-591.
- Markx, G.H., Talary, M. and Pethig, R. (1994b). Separation of viable and non-viable yeast using dielectrophoresis. *Journal of Biotechnology*, 32, 29-37.
- Markx, G.H. and Pethig, R. (1995). Dielectrophoretic of cells: Continuous separation. *Biotechnology Bioengineering*, 45, 337-343.
- Pethig, R. (1996). Dielectrophoresis: Using inhomogeneous AC electric fields to separate and manipulate cells. *Critical Reviews in Biotechnology*, 16(4), 331-348.
- Pethig, R. (1979). *Dielectric and Electronic Properties of Biological Materials*. J. Wiley and Sons.
- Pohl, H.A (1978). *Dielectrophoresis*. Cambridge, UK: Cambridge University Press.
- Suehiro, J., Zhou, G., Imamura, M. and Hara, M. (2003). Dielectrophoretic filter for separation and recovery of biological cells in water. *IEEE Transactions on Industry Applications*, 39(5), 1514-1521.